Propriétés statistiques des tremblements de terre

Etat de contrainte le long des zones de failles actives

Clément Narteau
P. Shebalin, S. Byrdina, M. Holschneider, D. Schorlemmer

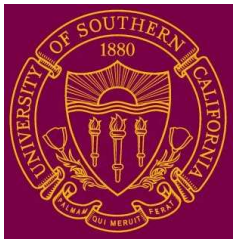

Dynamique des Fluides Géologiques, 8 Mars 2010

Statistical seismology

Statistical seismology is the science of making effective use of earthquake catalogues.

$\Downarrow$

Earthquake physics

Seismic hazard assessment

Geological description of earthquake faulting

$10^{-3}\ m$

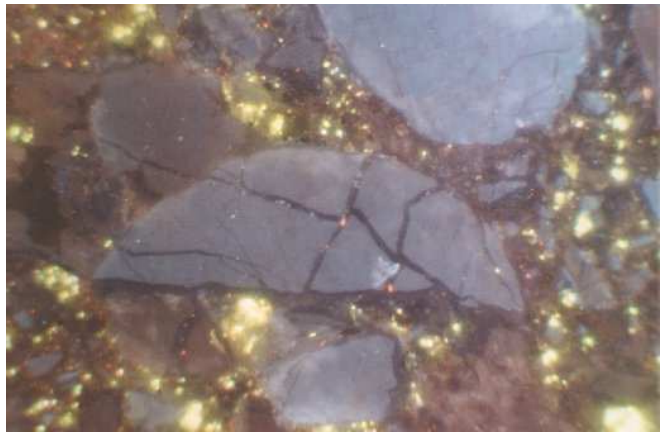

$10^{0}\ m$

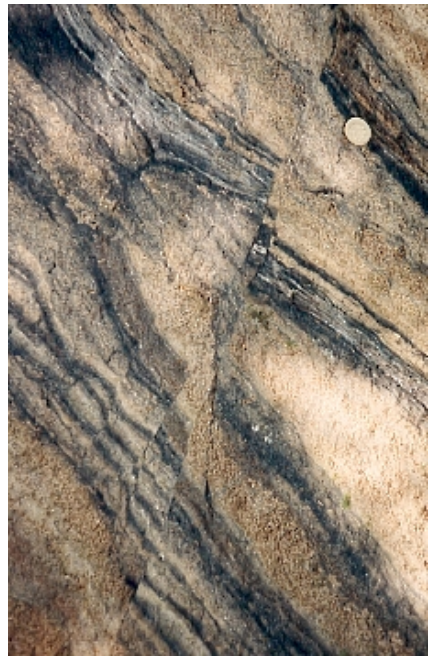

$10^{2}\ m$

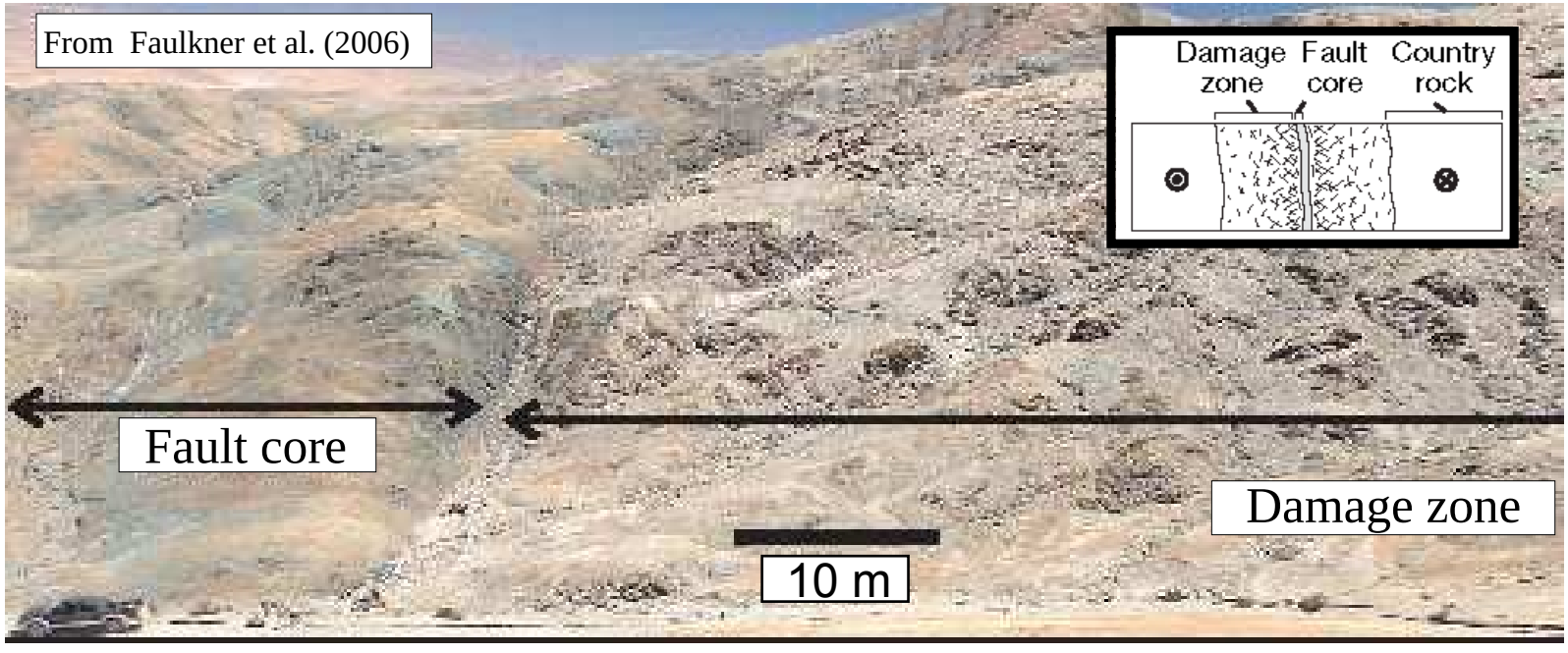

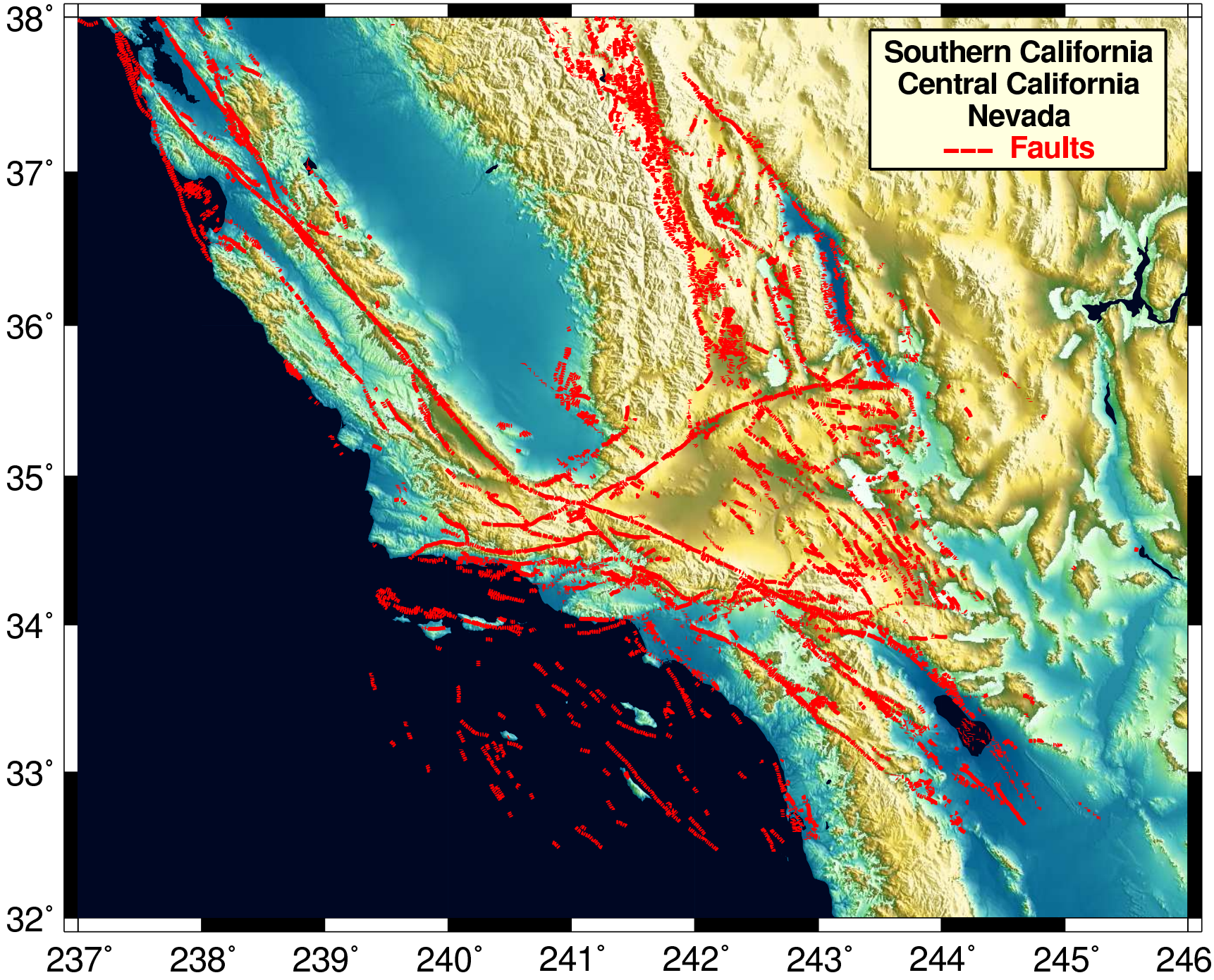
Southern California
Central California
Nevada
Faults
38°
37°
36°
35°
34°
33°
32°
237°
238°
239°
240°
241°
242°
243°
244°
245°
246°

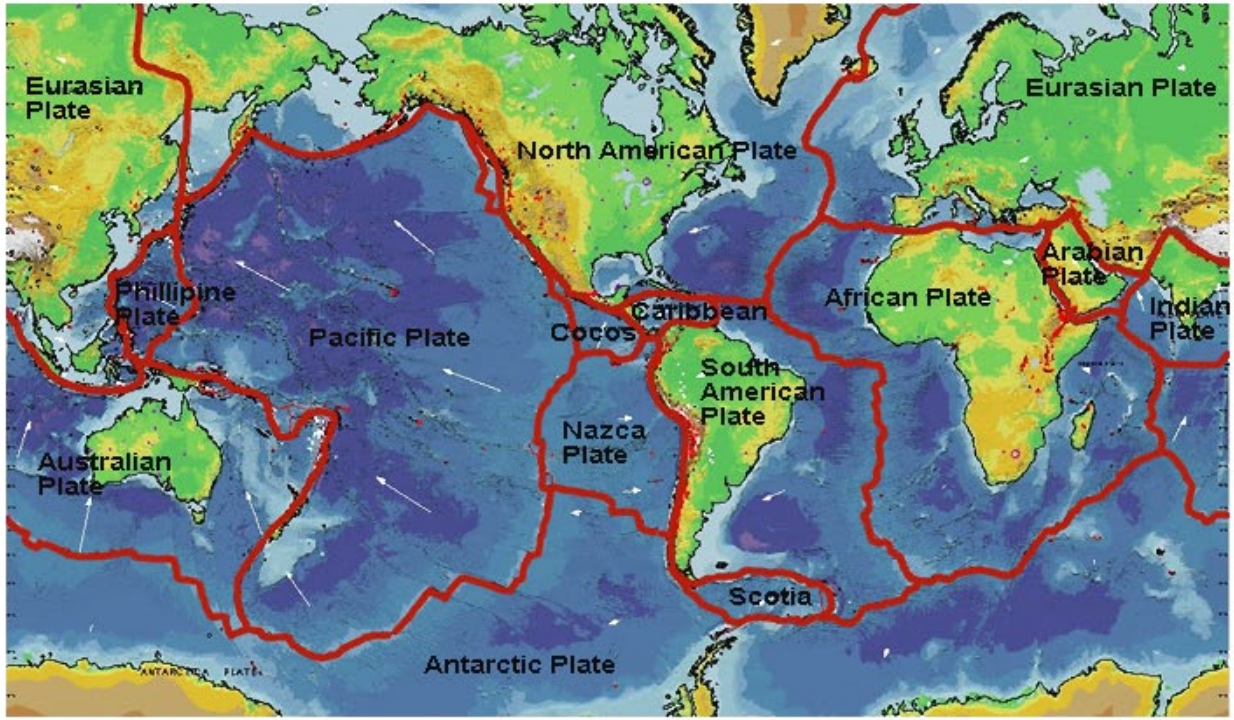
Eurasian Plate
North American Plate
Eurasian Plate
Arabian Plate
Phillipine Plate
Pacific Plate
Caribbean
Cocos
African Plate
Indian Plate
South American Plate
Nazca Plate
Australian Plate
Scotia
Antarctic Plate

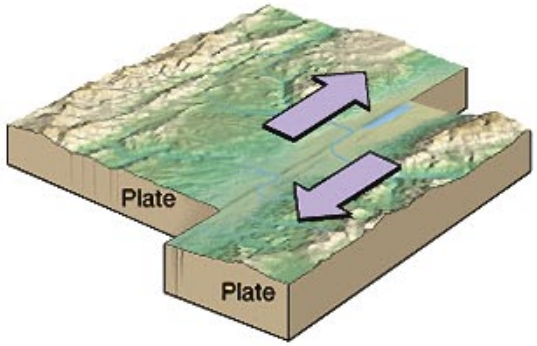
Plate
Plate

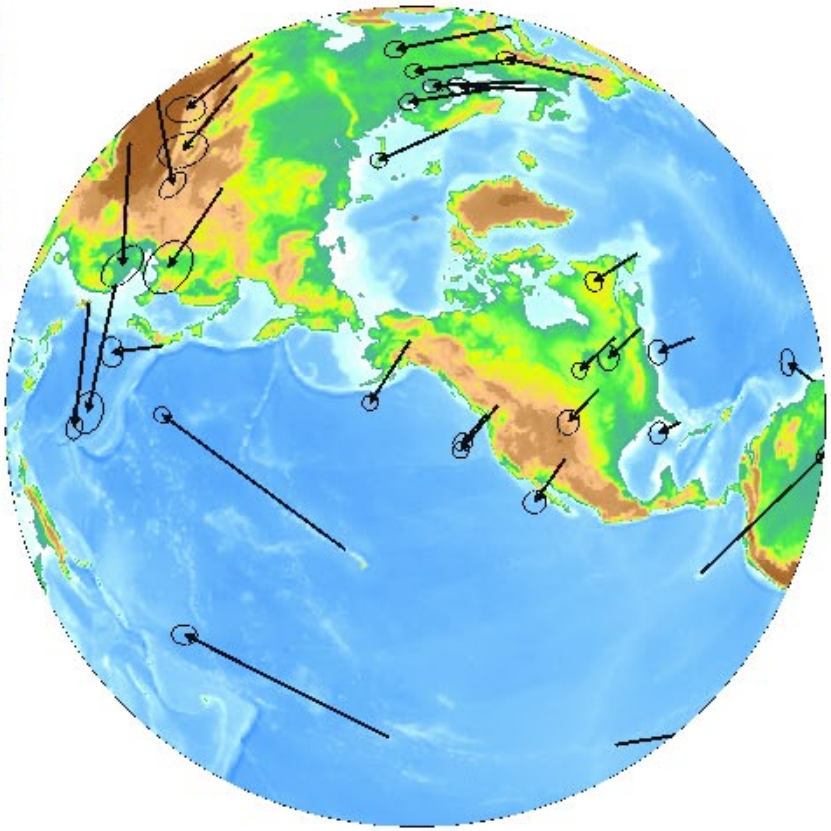

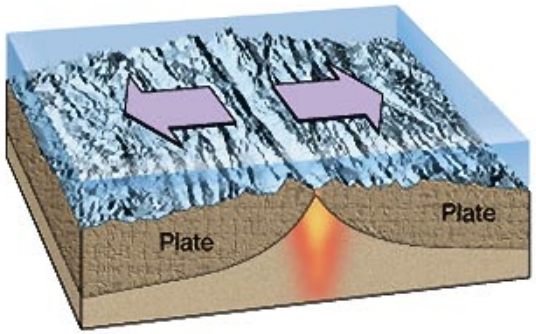
Plate
Plate

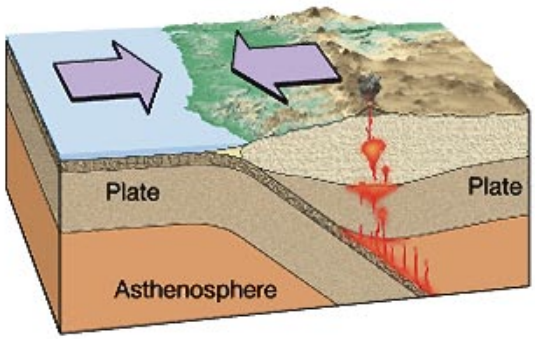
Plate
Plate
Asthenosphere

Faulting mechanism

Right-lateral
strike-slip faults

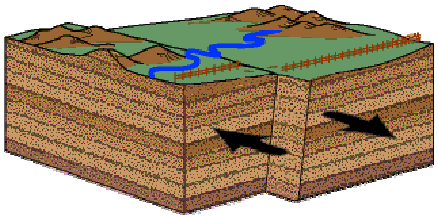

$rake = -180^o$

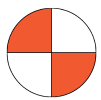

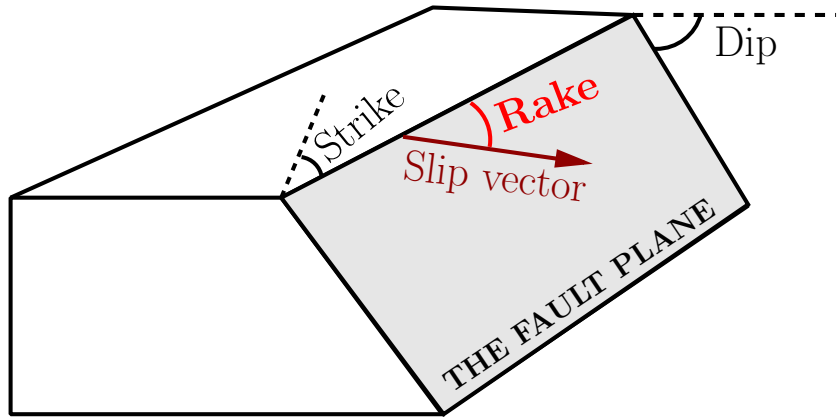

Right-lateral
strike-slip faults

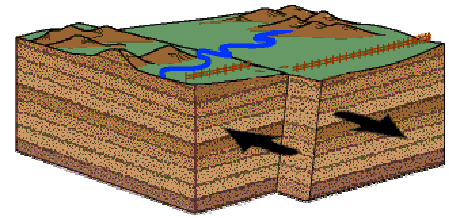

$rake = 180^o$

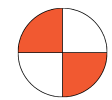

Normal faults

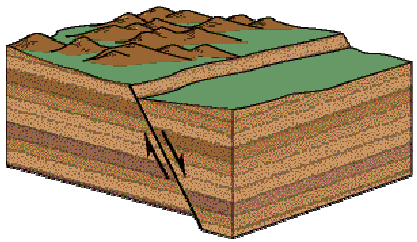

$rake = -90^o$

Left-lateral
strike-slip faults

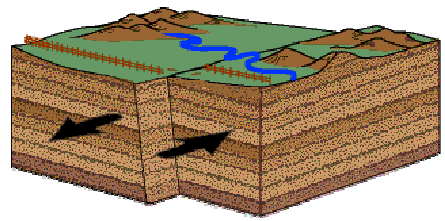

$rake = 0^o$

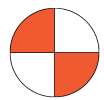

Thrust faults

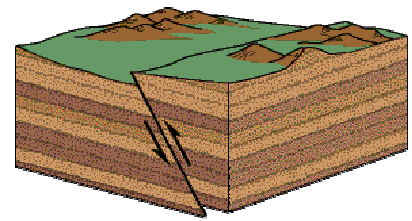

$rake = 90^o$

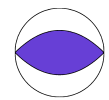

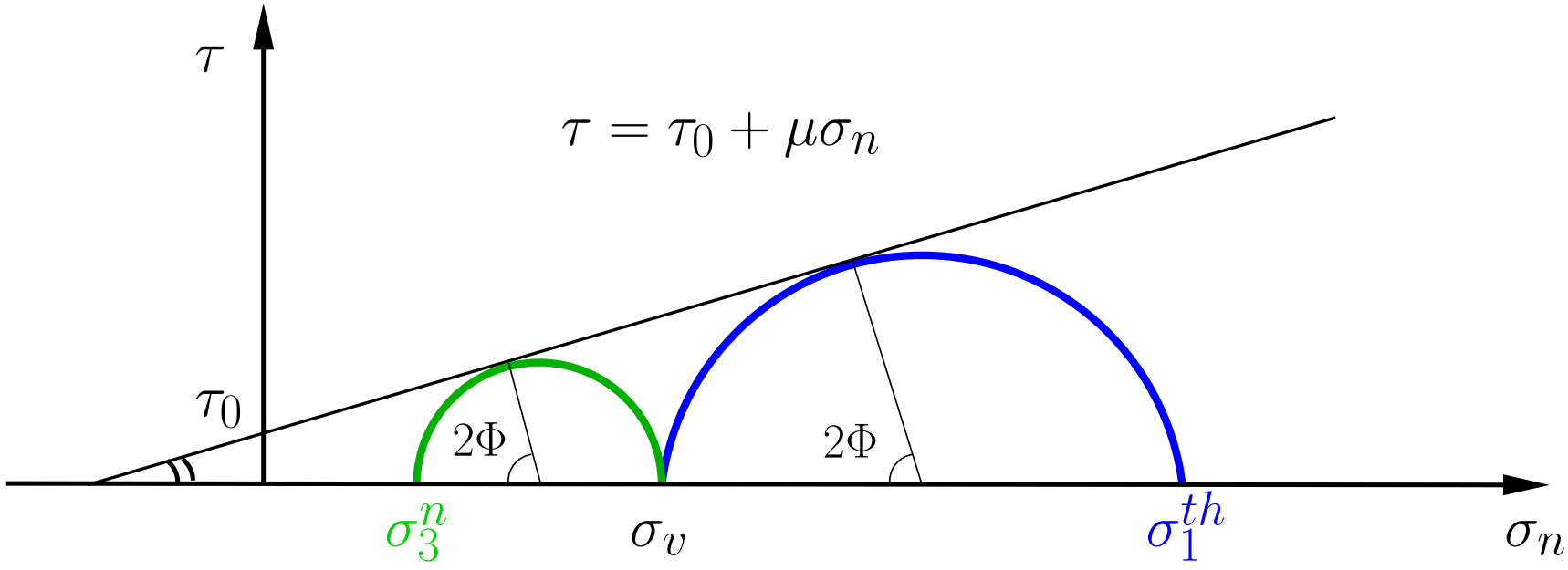

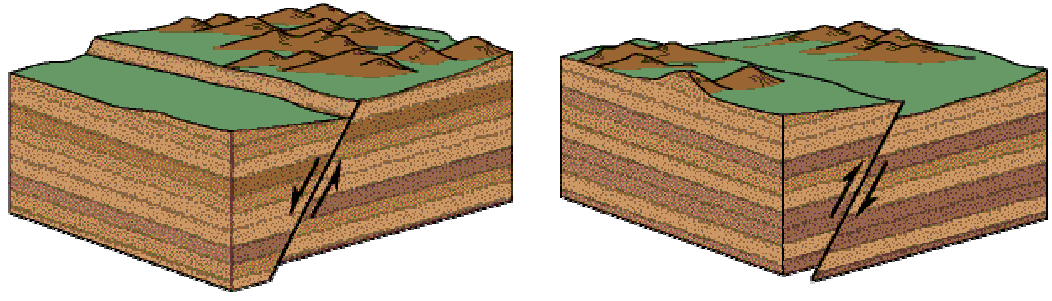

$\sigma_v = \sigma_1^n$ $\qquad$ $\sigma_v = \sigma_3^{th}$

$\Rightarrow$ $\qquad$ $\boxed{\sigma_1^n - \sigma_3^n < \sigma_1^{th} - \sigma_3^{th}}$

Normal faults

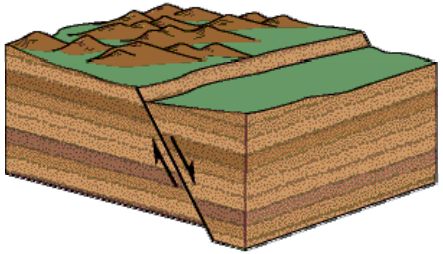

$rake = -90^o$

Left-lateral
strike-slip faults

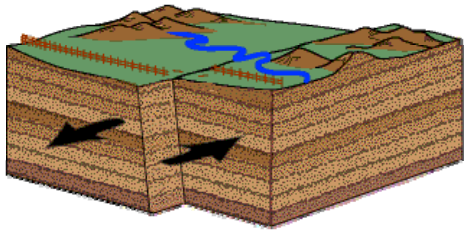

$rake = 0^o$

Thrust faults

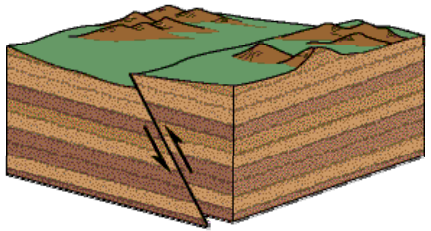

$rake = 90^o$

$$\sigma_1^n - \sigma_3^n \quad < \quad \sigma_1^{ss} - \sigma_3^{ss} \quad < \quad \sigma_1^{th} - \sigma_3^{th}$$

For $\mu = 0.75$, we have

$$\frac{\sigma_1^{th} - \sigma_3^{th}}{\sigma_1^n - \sigma_3^n} = 4 \qquad \frac{\sigma_1^{ss} - \sigma_3^{ss}}{\sigma_1^n - \sigma_3^n} = 1.6$$

Earthquake sequences

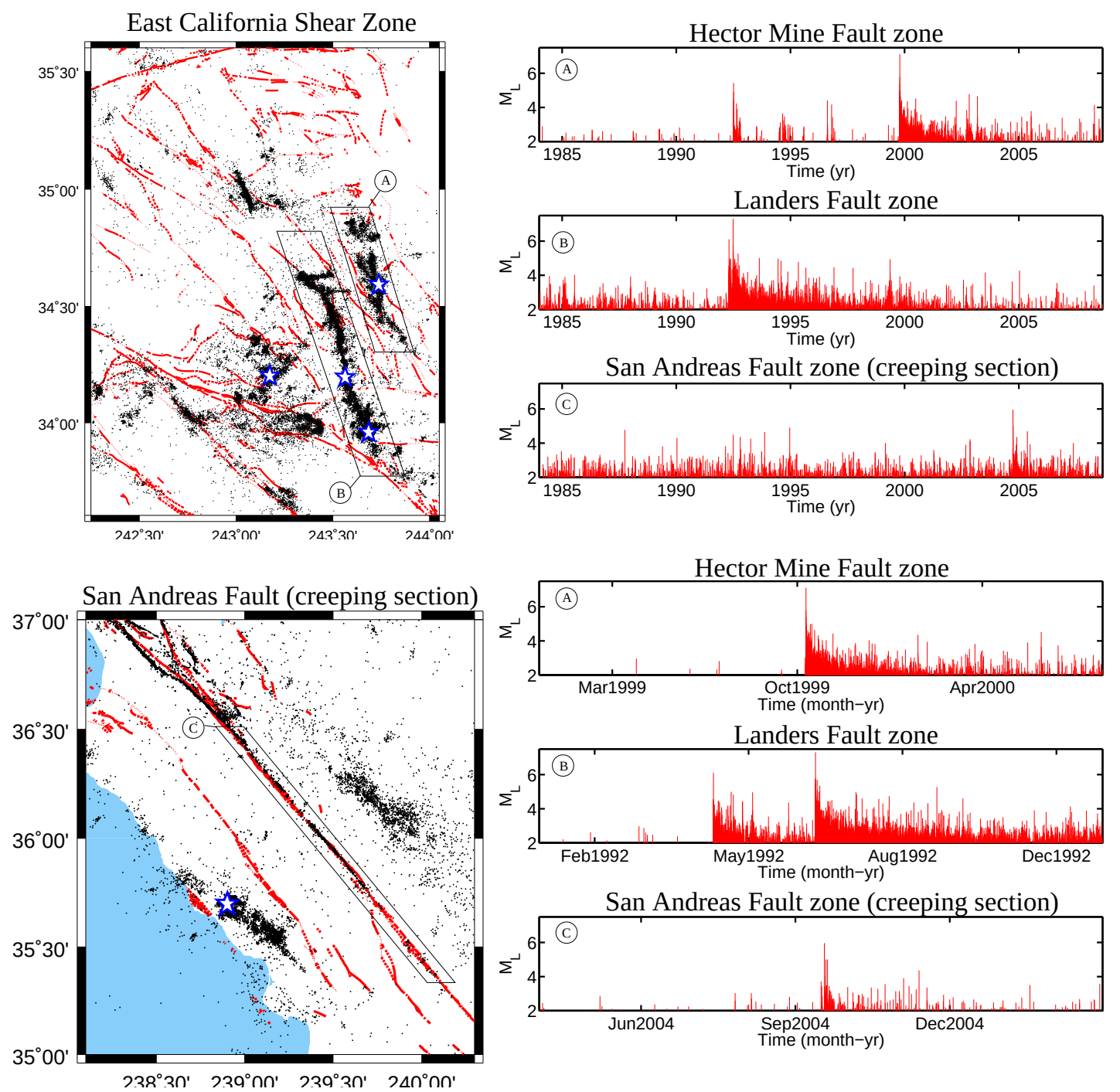
East California Shear Zone
35°30'
35°00'
34°30'
34°00'
242°30'
243°00'
243°30'
244°00'
A
B
Hector Mine Fault zone
Landers Fault zone
San Andreas Fault zone (creeping section)
M_L
Time (yr)
1985
1990
1995
2000
2005
San Andreas Fault (creeping section)
37°00'
36°30'
36°00'
35°30'
35°00'
238°30'
239°00'
239°30'
240°00'
C
Mar1999
Oct1999
Apr2000
Time (month−yr)
Feb1992
May1992
Aug1992
Dec1992
Jun2004
Sep2004
Dec2004

Earthquake sequences

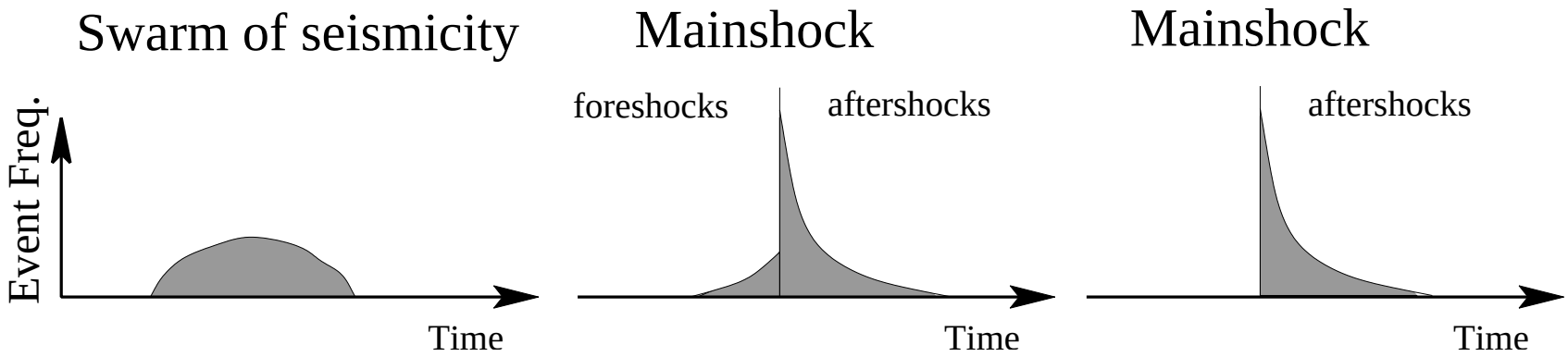

Foreshocks
Mainshocks
Aftershocks
Microseismicity

Empirical laws *Seismic cycle*

Statistical seismology

The frequency-size distribution

Gutenberg & Richter law

The aftershock decay rate

Modified Omori law

The frequency-size distribution

$$\log(N) = a - bM$$

M magnitude.
b slope of the frequency-size distribution.
a constant.

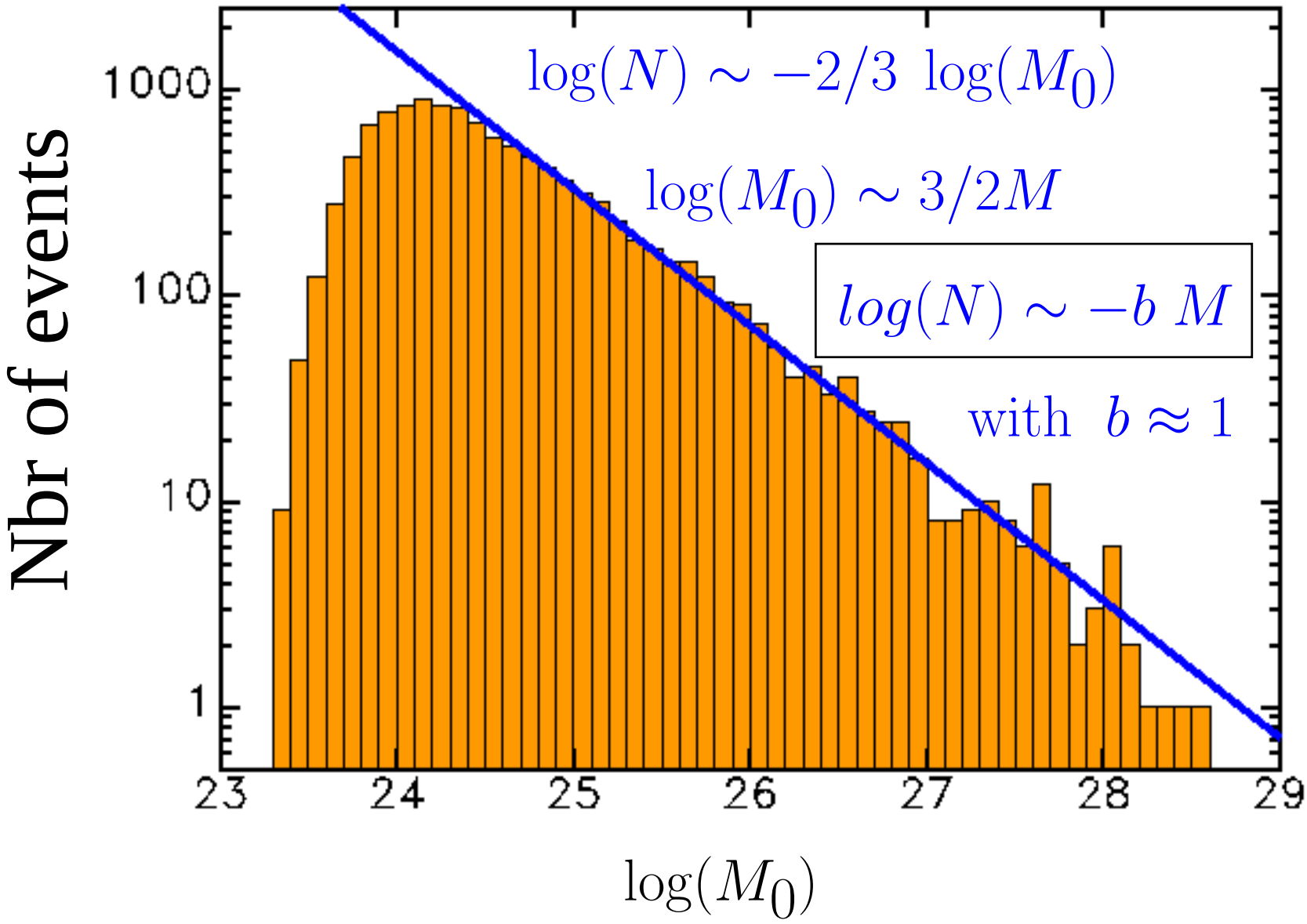
Nbr of events
1000
100
10
1
23
24
25
26
27
28
29
$\log(M_0)$
$\log(N) \sim -2/3\ \log(M_0)$
$\log(M_0) \sim 3/2M$
$log(N) \sim -b\ M$
with $b \approx 1$

The aftershock decay rate

$$\Lambda(t) = \frac{K}{(c+t)^p}$$

K	aftershock productivity.
t	elapsed time from the mainshock.
p	slope of the power law aftershock decay rate.
c	time delay before the onset of the power law aftershock decay rate.

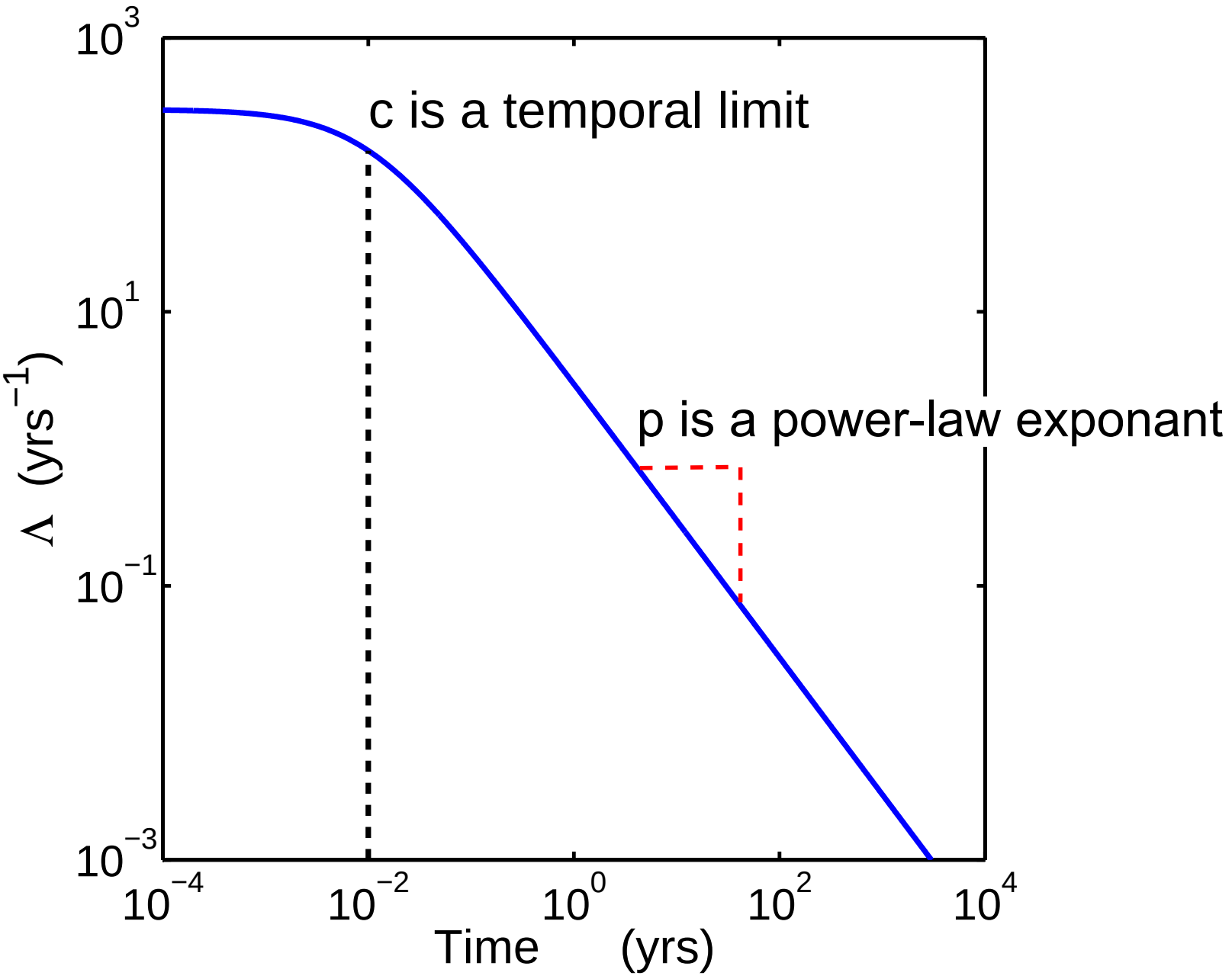
c is a temporal limit
p is a power-law exponant
10^3
10^1
10^{-1}
10^{-3}
Λ (yrs^{-1})
10^{-4}
10^{-2}
10^0
10^2
10^4
Time (yrs)

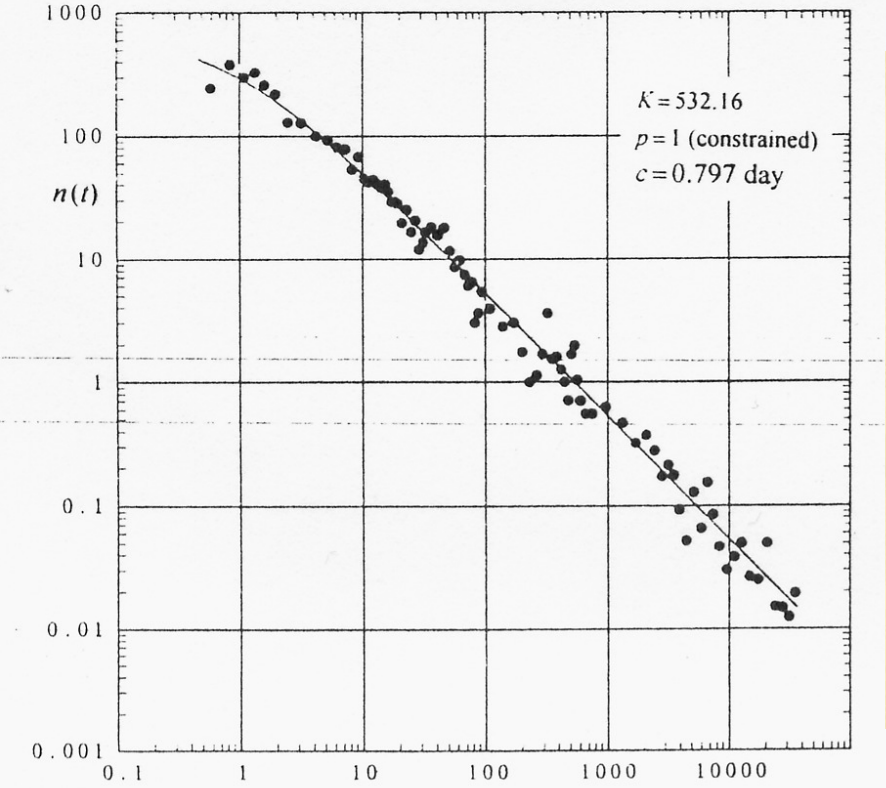

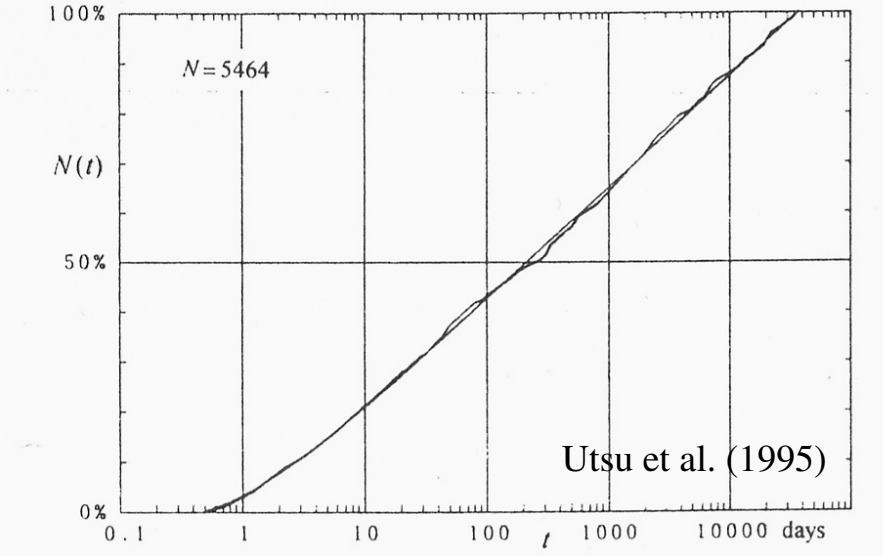

Utsu et al. (1995)

Nowadays

Are the statistical parameters controlled by geology ?

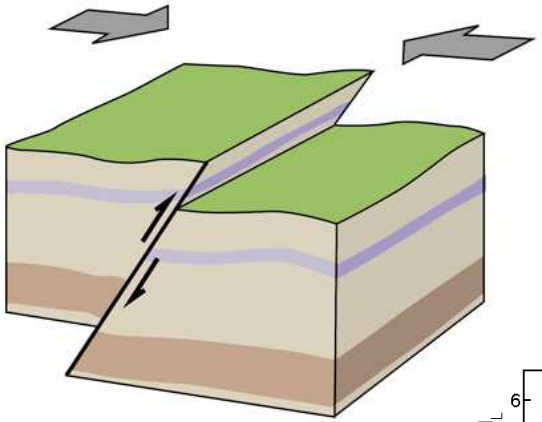

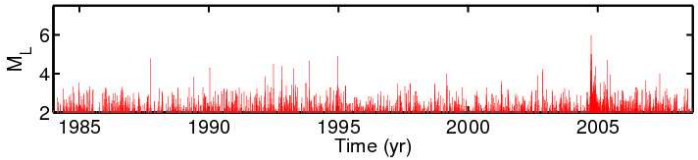

$$\Lambda(t) = \frac{K}{(c+t)^p}$$

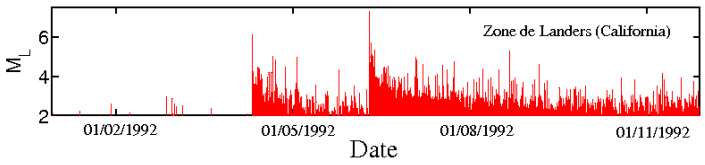

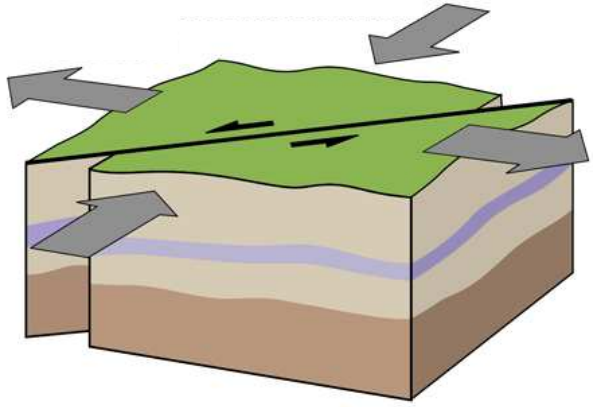

$$\log(N) = a - bM$$

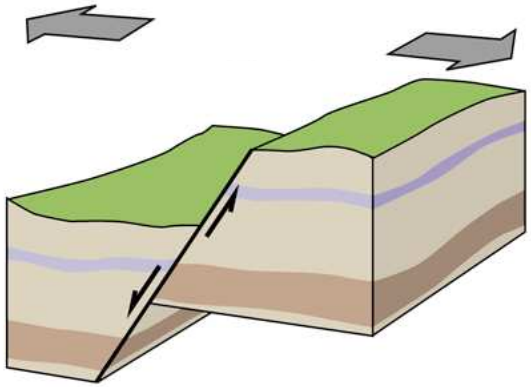

loading rate / seismic cycle

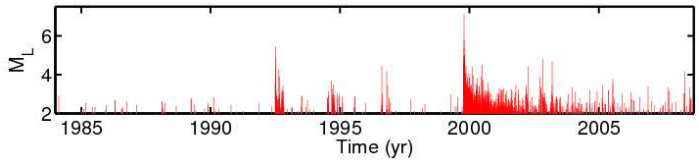

Statistical seismology across different stress regimes

We estimate

b-values

c-values

for different stress environments using moment tensor solutions in catalogues of seismicity.

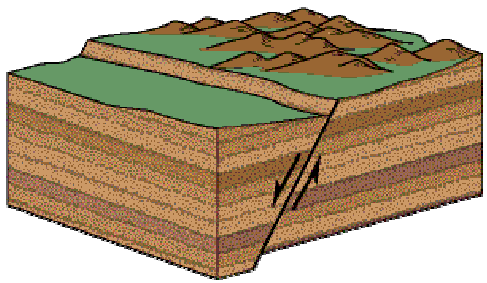
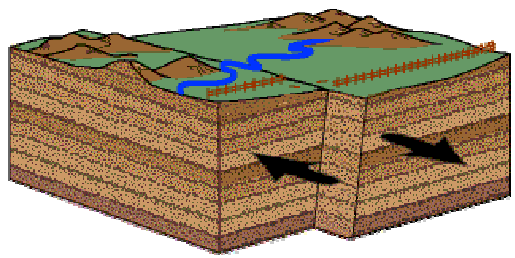
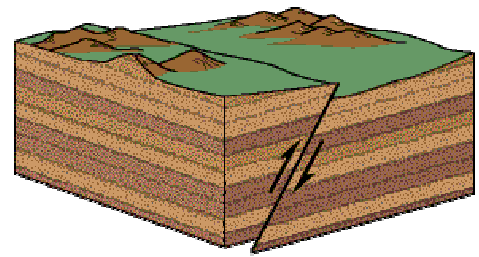

Earthquake Catalogues

- Location and time : $\{x, y, z, t\}$.
- Magnitude M.
- Faulting mechanism (3 parameters $\times 2$).
- Quality of the record.
- Reference number.

The completeness issue

- The studied area.
- The duration of the study.
- The origin of the signal (volcanic seismicity).

The different catalogues

Network	Period	M_c	Depth (km)	No. of events
Harvard CMT	1.1.1980–31.12.2004	5.5	0–50	7,636
SCSN	1.1.1981–31.12.2003	2.5	all	14,003
NCSN	1.1.1981–31.12.2004	3.0	all	4,250
NEID F-Net	4.1.1997–31.12.2004	4.5	0–50	1,579
NEID Kanto-Tokai	1.1.1982–1.7.2003	3.0	0–50	2,337

Schorlemmer et al. (2005)

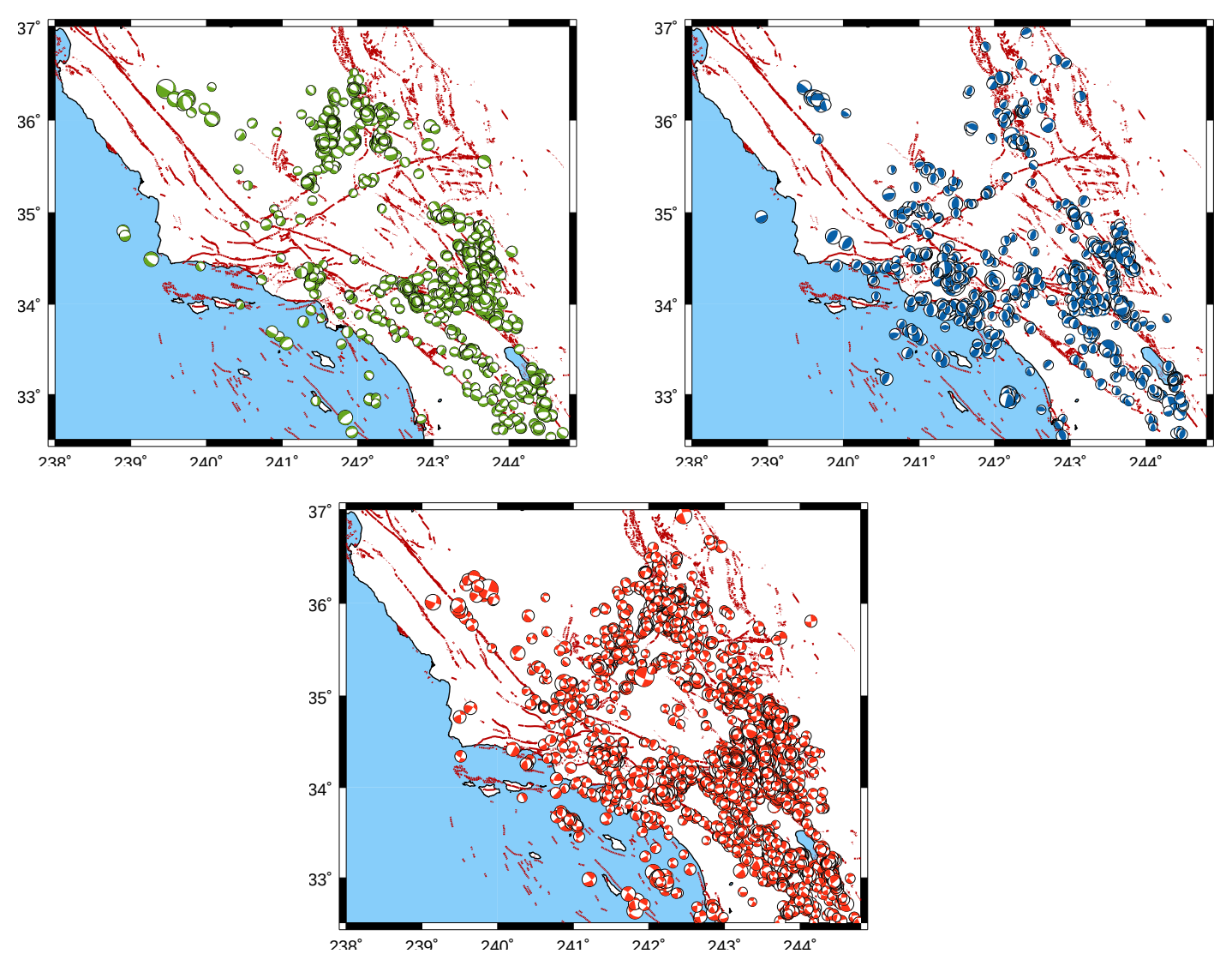
37°
36°
35°
34°
33°
238°
239°
240°
241°
242°
243°
244°

The frequency-size distribution

$$\log(N) = a - bM$$

M magnitude.
b slope of the frequency-size distribution.
a constant.

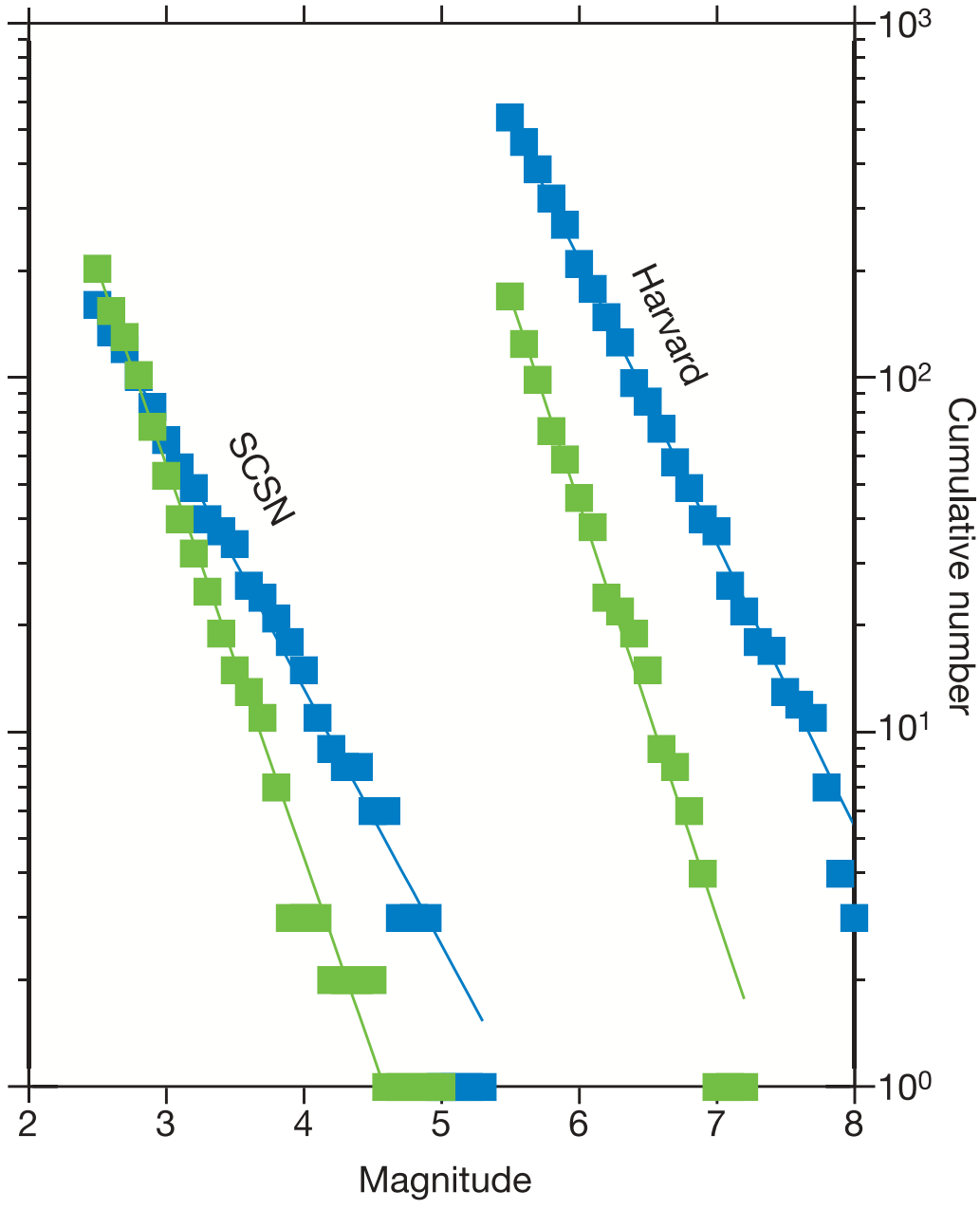

Schorlemmer et al. (2005)

The b-values for 3 classes of rakes

Network	Range γ (deg)	b_{TH}	b_{SS}	b_{NR}
SCSN	05	0.72 ± 0.05	1.00 ± 0.05	1.11 ± 0.08
	25	0.75 ± 0.03	0.87 ± 0.01	1.07 ± 0.04
	45	0.79 ± 0.02	0.87 ± 0.01	1.03 ± 0.03
Harvard	05	0.81 ± 0.03	1.13 ± 0.05	1.17 ± 0.08
	25	0.89 ± 0.02	0.99 ± 0.02	1.12 ± 0.04
	45	0.93 ± 0.02	0.98 ± 0.02	1.17 ± 0.04
NCSN	05	-	-	-
	25	0.67 ± 0.05	0.81 ± 0.02	1.01 ± 0.06
	45	0.73 ± 0.04	0.91 ± 0.02	1.00 ± 0.04
Kanto-Tokai	05	-	-	-
	25	0.68 ± 0.03	0.89 ± 0.05	1.03 ± 0.09
	45	0.66 ± 0.02	0.90 ± 0.04	1.06 ± 0.07
F-Net	05	-	-	-
	25	0.80 ± 0.04	1.02 ± 0.07	1.06 ± 0.08
	45	0.78 ± 0.03	1.09 ± 0.05	1.05 ± 0.05

Schorlemmer et al. (2005)

The b-values for different rake angles

Earthquakes are redistributed in 73 classes according to their rake angles.

Each class has a width of 40^{o} from -180^{o} to 180^{o} by step of 5^{o}.

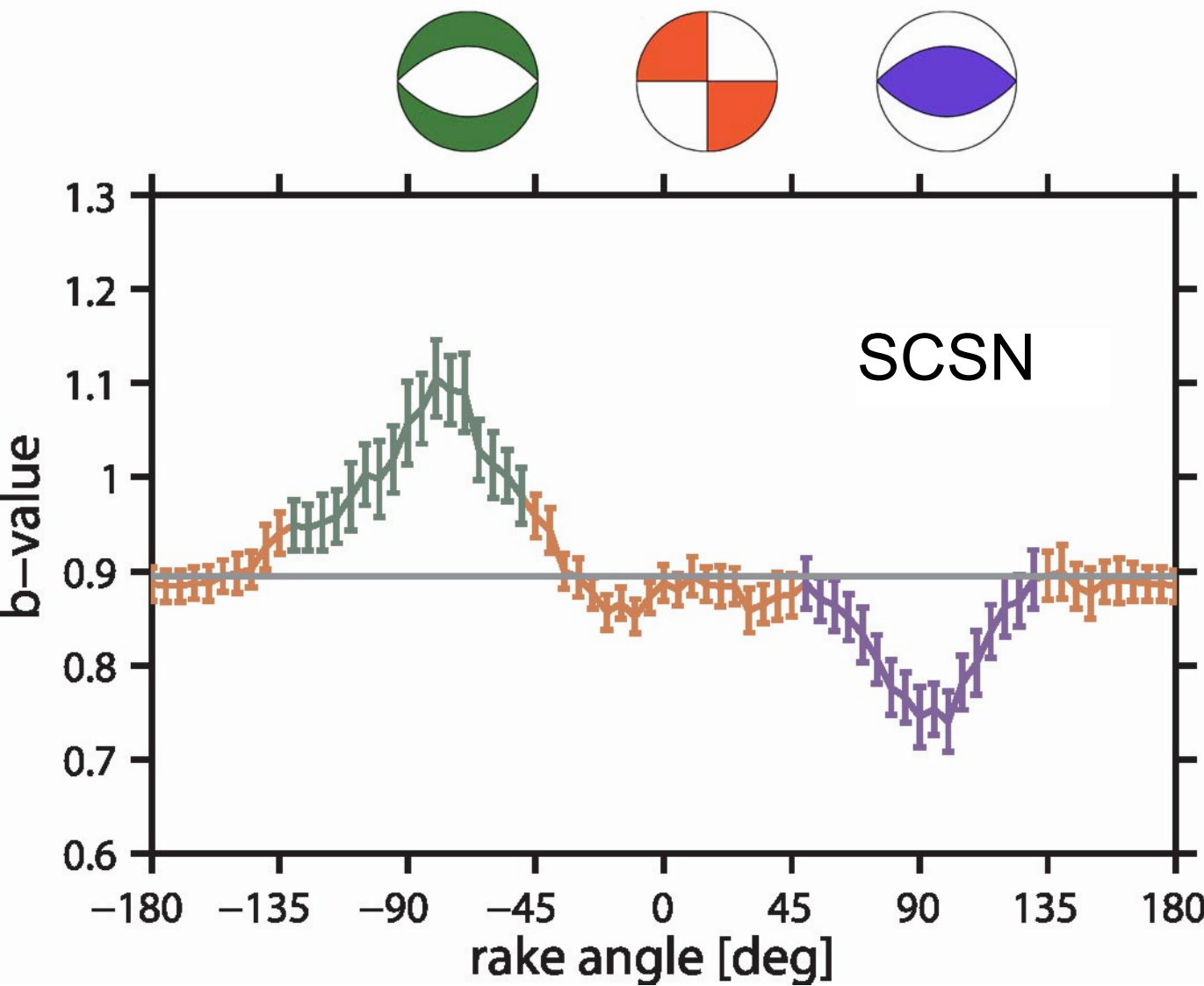
SCSN
b–value
1.3
1.2
1.1
1
0.9
0.8
0.7
0.6
–180
–135
–90
–45
0
45
90
135
180
rake angle [deg]

Partial conclusion

There is a positive correlation between the differential shear stress and the fractal dimension of distributed seismicity.

The aftershock decay rate

$$\Lambda(t) = \frac{K}{(c+t)^p}$$

K	aftershock productivity.
t	elapsed time from the mainshock.
p	slope of the power law aftershock decay rate.
c	time delay before the onset of the power law aftershock decay rate.

What is an aftershock ?

There is no unique way of differenciating between mainshocks, foreshocks and aftershocks.

$\Downarrow$

No precise definition of an aftershock

$\Downarrow$

Here, an aftershock is an earthquake,
occuring in the neighbourhood of a larger magnitude event according to a given space-time window.

A declustering method

To identify mainshocks, we deselect earthquakes which are within a

$$R_w(m) = 0.020 \cdot 10^{0.50m}$$

kilometer radius circle during the first

$$T_w(m) = 0.125 \cdot 10^{0.55m}$$

days after an event of magnitude m. Using the same spatial scaling, we deselect mainshocks that precede larger events by less than 12 hours.

Then, we investigate the existence of nonzero c-values by varying magnitude thresholds for mainshocks and aftershocks

$$(M^{\mathrm{A}}_{\mathrm{Min}},\ M^{\mathrm{A}}_{\mathrm{Max}}) \qquad (M^{\mathrm{M}}_{\mathrm{Min}},\ M^{\mathrm{M}}_{\mathrm{Max}})$$

Magnitude thresholds for mainshocks

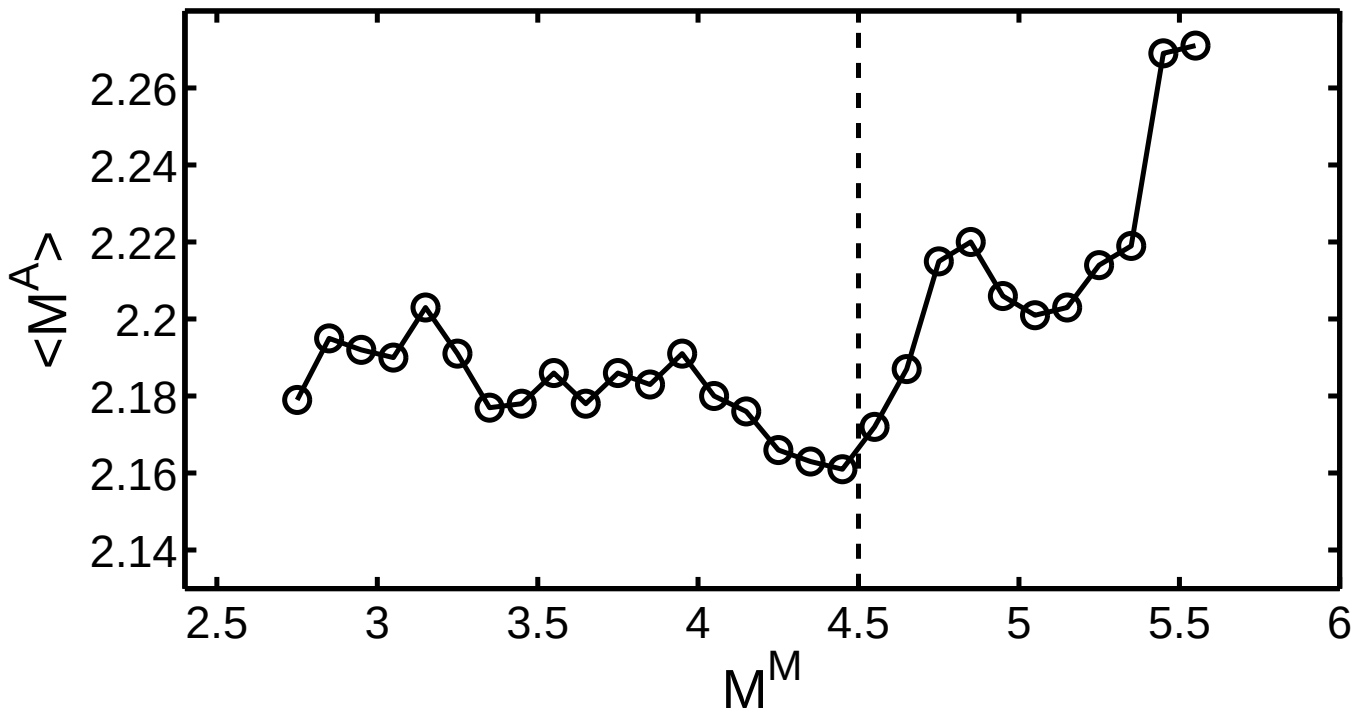

$M^M_{Min} = 2.5$ $M^M_{Min} = 4.5$

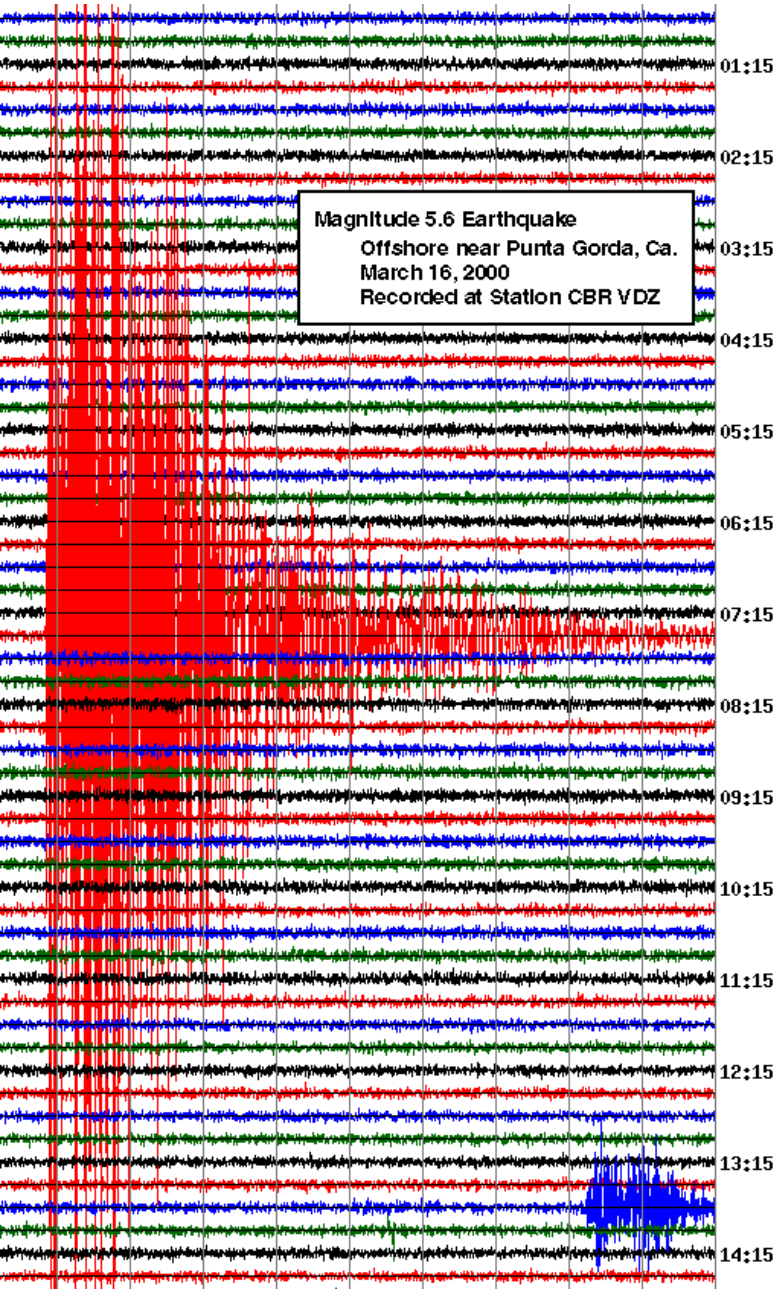
Magnitude 5.6 Earthquake
Offshore near Punta Gorda, Ca.
March 16, 2000
Recorded at Station CBR VDZ
01:15
02:15
03:15
04:15
05:15
06:15
07:15
08:15
09:15
10:15
11:15
12:15
13:15
14:15

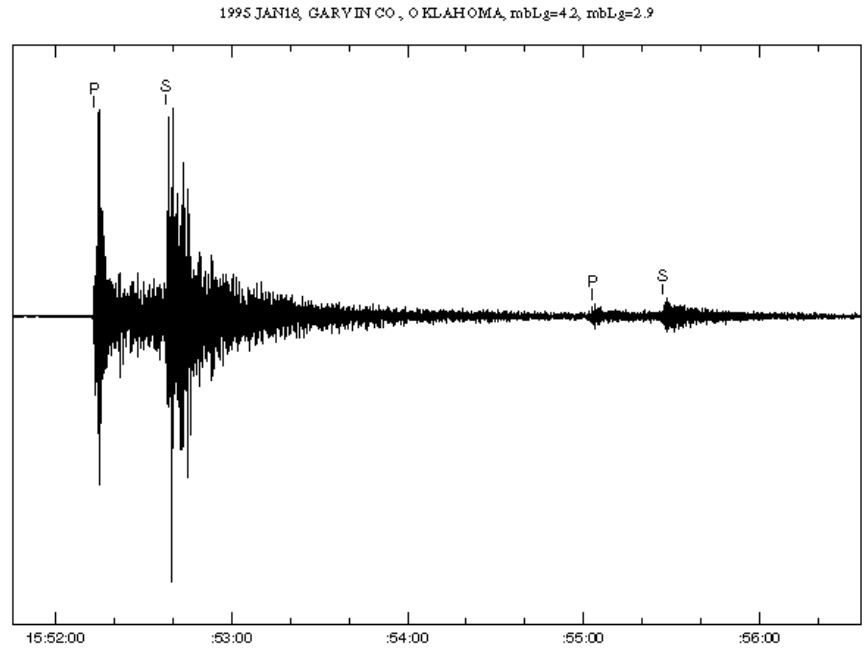
1995 JAN18, GARVIN CO., O KLAHOMA, mbLg=4.2, mbLg=2.9
P
S
P
S
15:52:00
:53:00
:54:00
:55:00
:56:00
Time (hr:min:sec) UTC/GMT

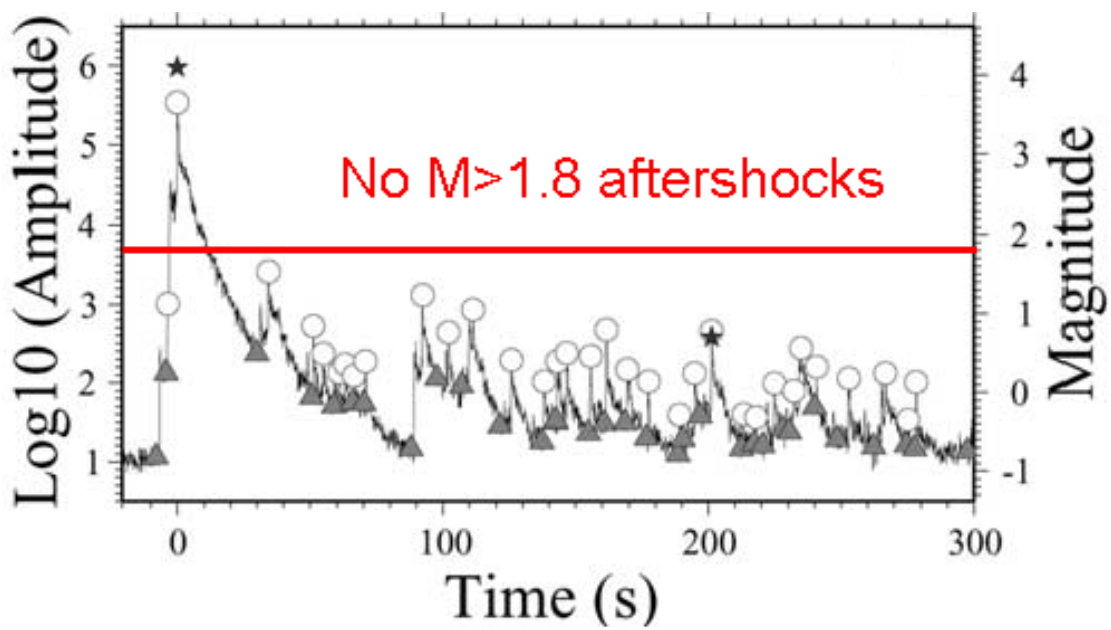
No M>1.8 aftershocks
Log10 (Amplitude)
Magnitude
Time (s)
0
100
200
300
1
2
3
4
5
6
-1
0
1
2
3
4

Magnitude thresholds for aftershocks

Aftershocks are stacked according to the times from their repective mainshock. Then, for different range of magnitude, c-values are calculated by a maximum likelihood method.

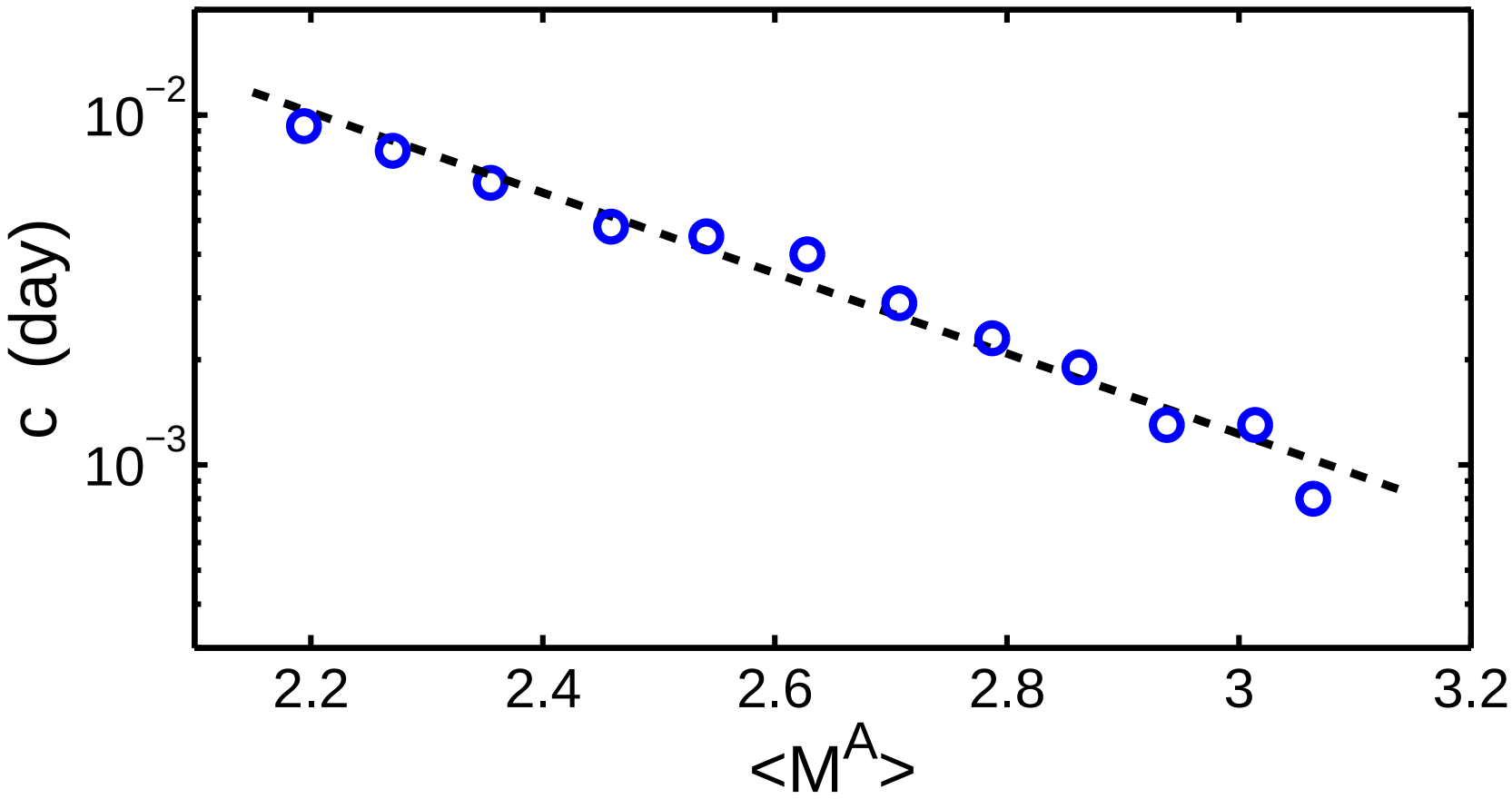

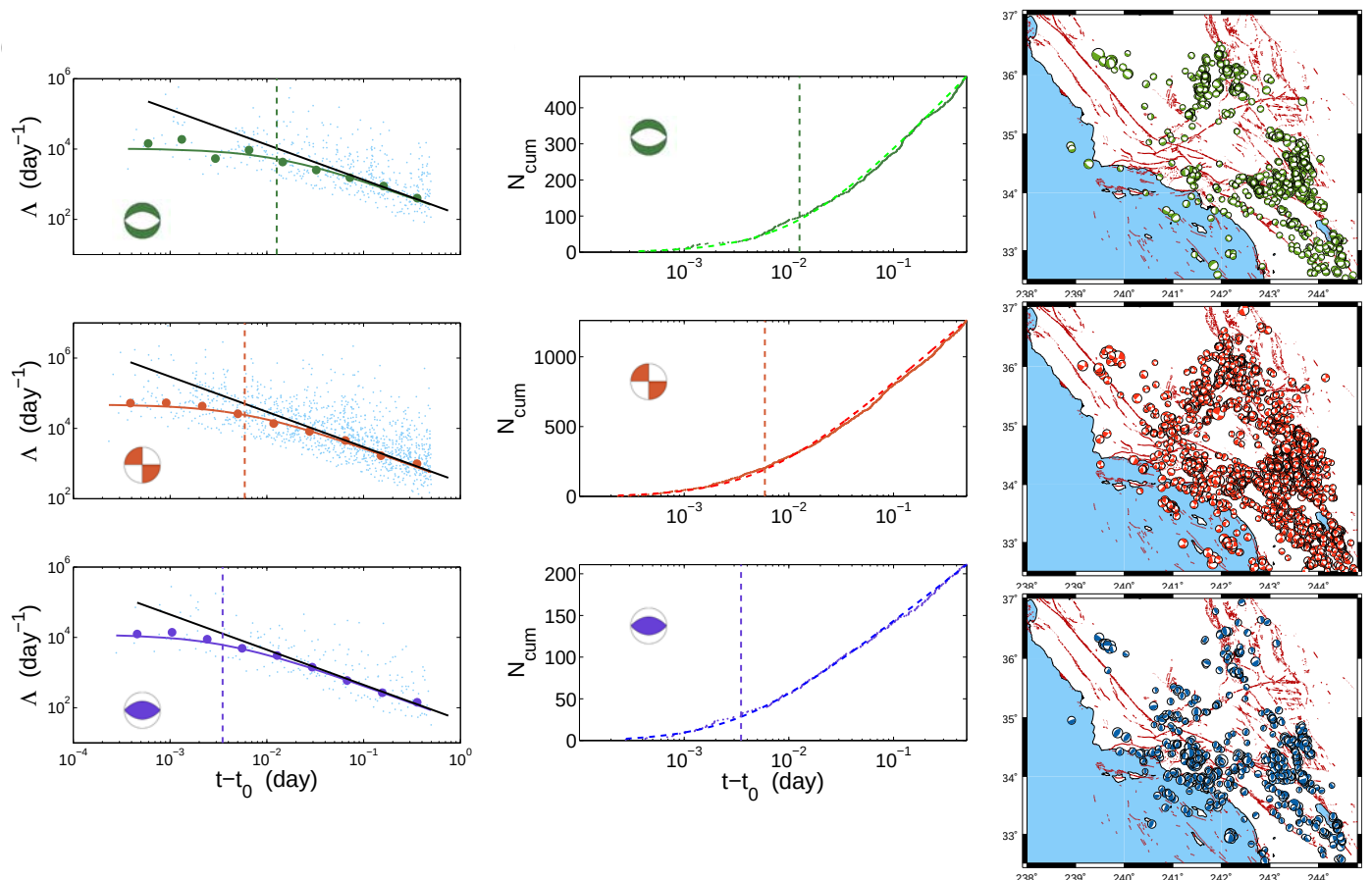
Λ (day^{-1})
10^6
10^4
10^2
10^{-4}
10^{-3}
10^{-2}
10^{-1}
10^0
t−t$_0$ (day)
N$_{cum}$
0
100
200
300
400
500
1000
50
150
37°
36°
35°
34°
33°
238°
239°
240°
241°
242°
243°
244°

Evaluation of c-values

The c-value depends on earthquake magnitude.

Then, for different ranges of magnitude, aftershocks are separated in 73 classes according to the rake angle of their respective mainshock. In each class, events are merged together in a stack taking $t = 0$ the time of the mainshock.

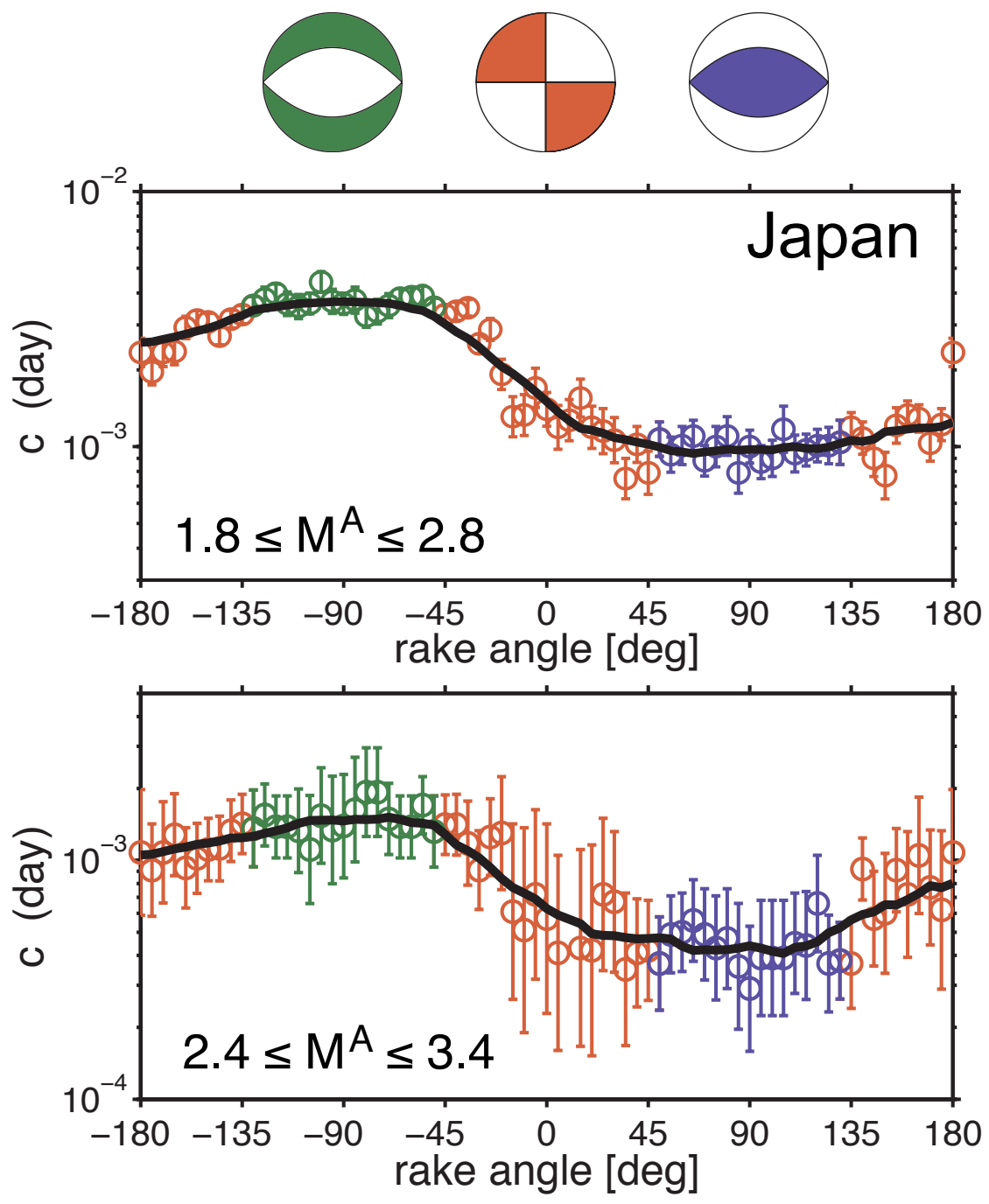
Japan
10^{-2}
10^{-3}
c (day)
$1.8 \leq M^A \leq 2.8$
−180 −135 −90 −45 0 45 90 135 180
rake angle [deg]
10^{-3}
10^{-4}
c (day)
$2.4 \leq M^A \leq 3.4$
−180 −135 −90 −45 0 45 90 135 180
rake angle [deg]

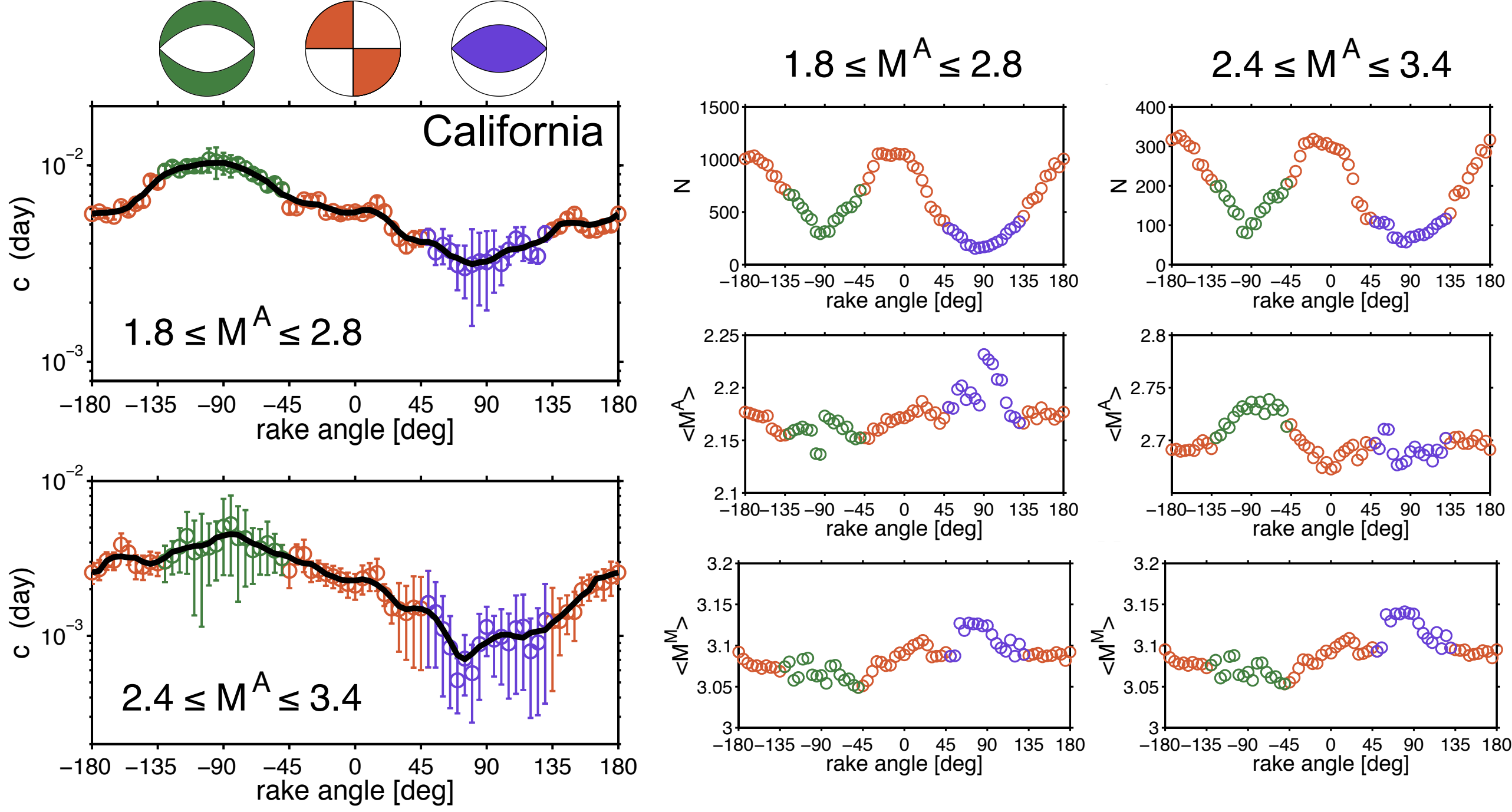
California
1.8 ≤ M^A ≤ 2.8
2.4 ≤ M^A ≤ 3.4
c (day)
rake angle [deg]
N
<M^A>
<M^M>

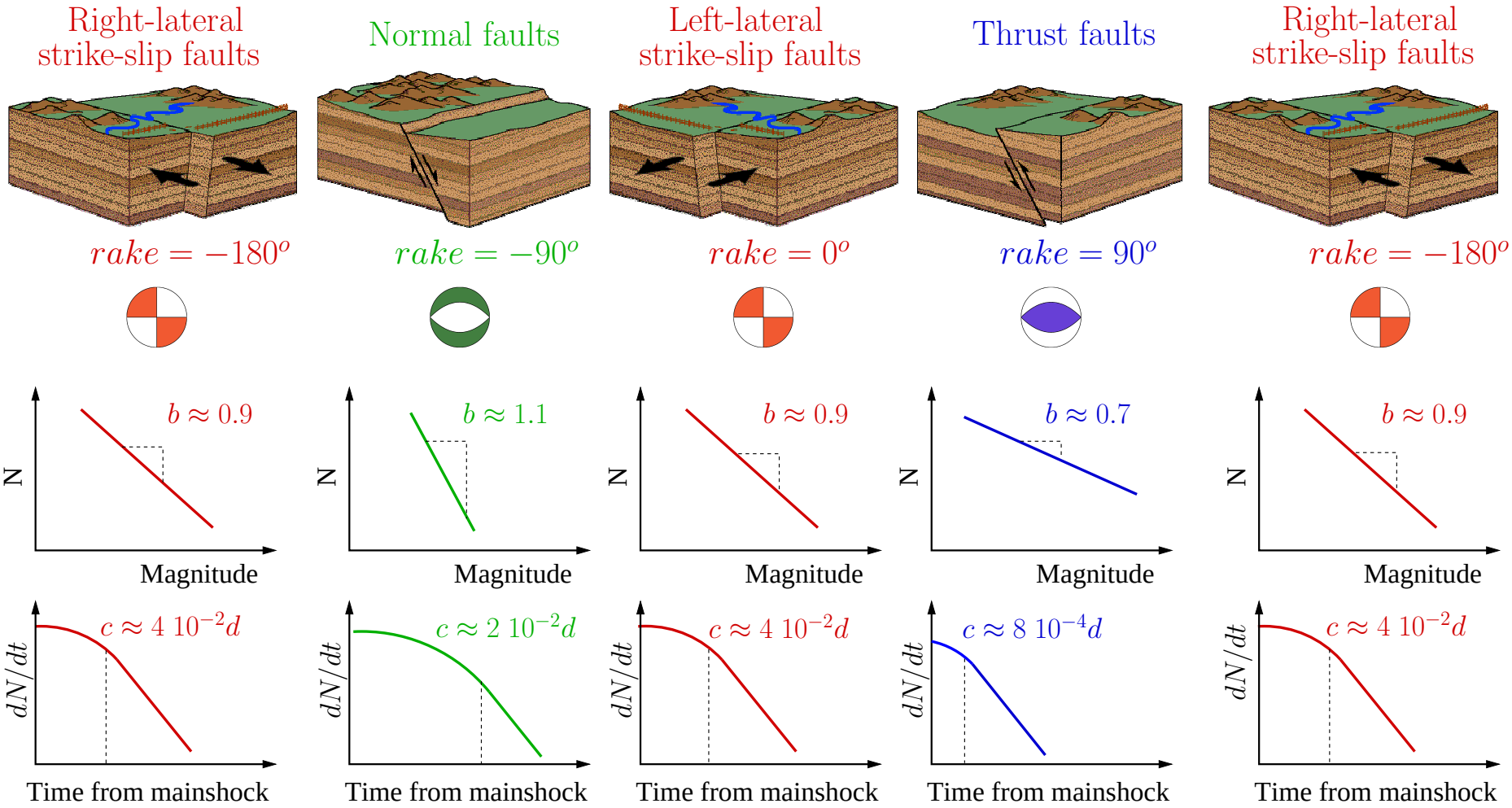

$$\sigma_1^n - \sigma_3^n \quad < \quad \sigma_1^{ss} - \sigma_3^{ss} \quad < \quad \sigma_1^{th} - \sigma_3^{th}$$

A common dependency on stress

The b-value determines the ratio between the number of large and small earthquakes and its variations can be associated with the ability for an earthquake rupture to propagate (lower b-value) or not (higher b-value).

The c-value is the time delay required to reach a steady relaxation regime.

Process zone fracturing

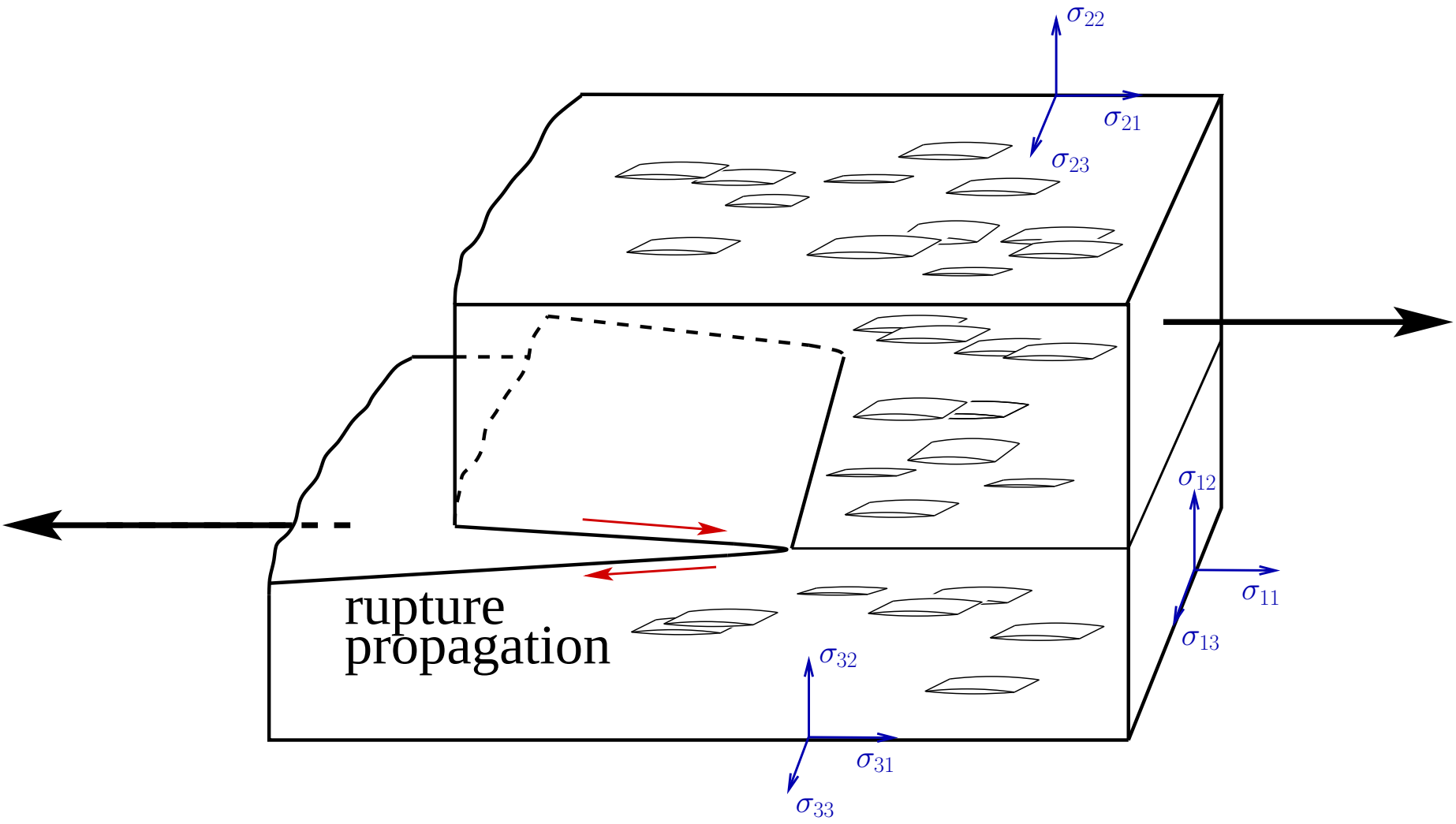

Nucleation of aftershocks

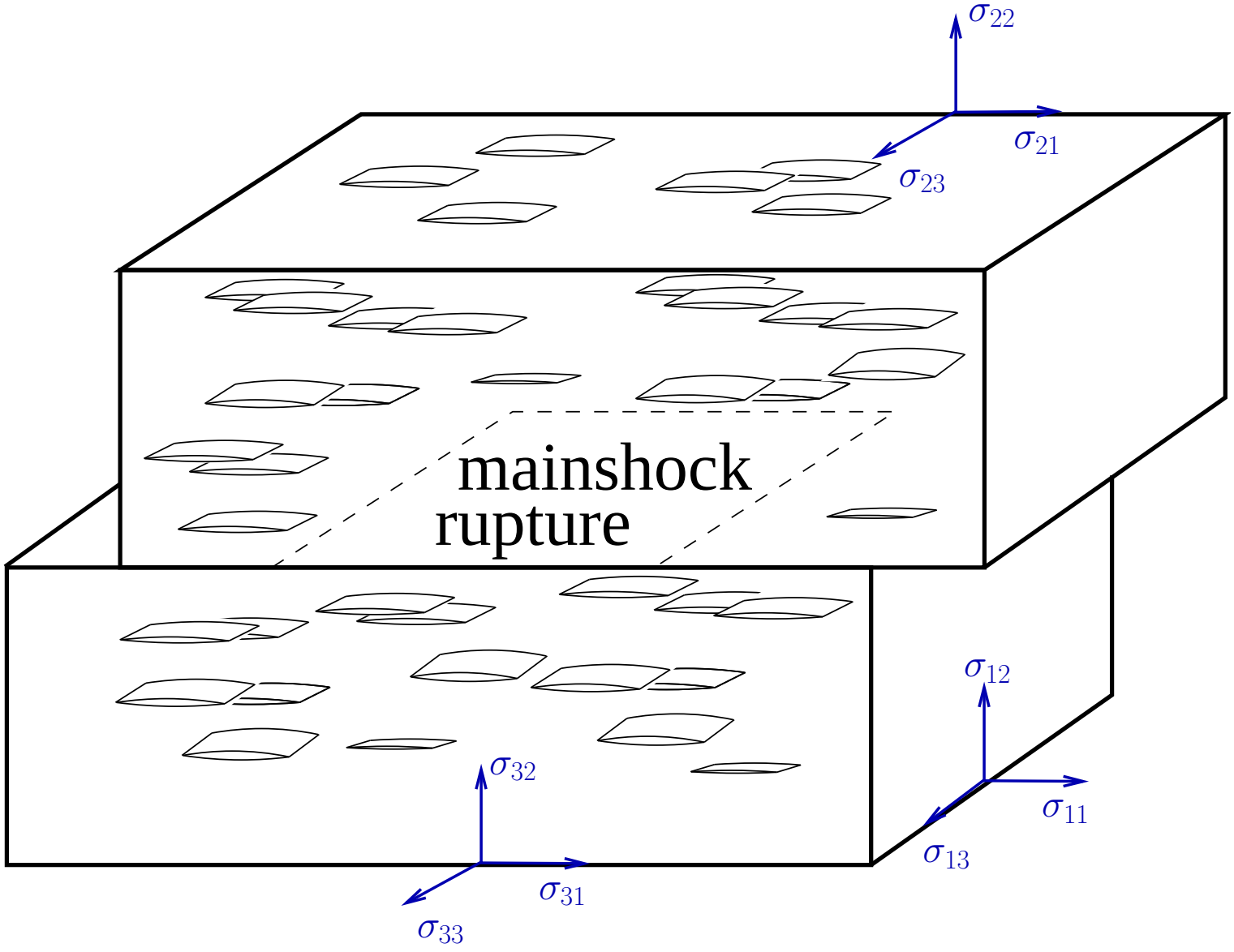

Conclusions

- As an example, we have shown that the aftershock decay rate and the frequency-size distribution exhibit similar dependency on stress.
- Changes in power laws can be related to the mechanics of faulting over short and long time scales.
- This indicates a common time-dependent behavior of fracturing during the propagation of earthquakes and for the nucleation of aftershocks.

Perspectives

- Alarm-based models from Early aftershock statistics.
- Estimation of the strain accumulation rate in different active-tectonic regions :

$\longrightarrow$ Creeping section.

$\longrightarrow$ Locked section.